IUST International Journal of Engineering Science,
Vol. 19, No.5-1, 2008, Page 105-113

THERMAL BEHAVIOR ANALYSIS OF THE FUNCTIONALLY GRADED TIMOSHENKO'S BEAM

GH. Rahimi & AR. Davoodinik

Abstract: *The intention of this study is the analysis of thermal behavior of functionally graded beam (FGB). The distribution of material properties is imitated exponential function. For thermal loading the steady state of heat conduction with exponentially and hyperbolic variations through the thickness of FGB, is considered. With comparing of thermal behavior of both isotropic beam and FGB, it is appeared that the quality of temperature distribution plays very important part in thermal resultant distribution of stresses and strains for FGB. So that, for detecting the particular thermal behavior of FGB, the function of heat distribution must be same as function of material properties distribution. In addition, In the case of exponential distribution of heat with no mechanical loads, in spite of the fact that the bending is accrued, the neutral surface does not come into existence.*

Keywords: *Timoshenko's beam, exponentially distribution, functionally graded material, thermal behavior*

1. Introduction

Functionally graded materials (FGMs) have been researched and developed in many engineering fields that need to be super heat resistant, such as the outer wall and the engine parts of future space-planes. In FGMs, material properties vary continuously from one surface to the other, especially from metal to ceramic. From this continuous change in composition, FGMs can withstand high-temperature environments while maintain their structural integrity. Due to these advantages, various researches have been tried about the modeling and application of FGMs for plates and shells that subjected to thermal loads. Javaheri and Eslami derived the equilibrium and stability equations of a functionally graded rectangular plate under thermal loads, based on the classical plate theory. Buckling analysis of FGM plates under four types of thermal loads was carried out in closed-form solutions [1].

Najafizadeh and Eslami analyzed the thermal buckling of FGM circular plates under three types of thermal loads. The nonlinear equilibrium and linear stability equations were derived using variation formulations [2]. Shen studied a post buckling analysis for a functionally graded cylindrical panel of finite length subjected to axial compression in thermal environments. Material properties were assumed to be temperature dependent, and graded in the thickness direction according to a simple power law distribution. The governing equations were based on Reddy's higher order shear deformation shell theory with a von Karman–Donnell-type of kinematic nonlinearity and including thermal effects [3]. The thermal buckling behavior under uniform or non-uniform temperature rise was analyzed; however, the time-dependent temperature rise was not considered [4]. Kyung and Kim studied three-dimensional thermo-mechanical buckling analysis for functionally graded composite structures that composed of ceramic, functionally graded material (FGM), and metal layers. The finite element model is adopted by using an 18-node solid element to analyze more accurately the variation of material properties and temperature field in the thickness direction. For a time discretization, Crank–Nicholson method is used [5].

Ravichandran examined the effects of the functional form of gradation including the presence and structural arrangement of monolithic Al_2O_3–Ni regions in combination with the graded region, on the thermal residual stresses, arising from the fabrication of a FGM system [6]. However, for functionally graded beams (FGB), related studies are very limited. Sankar established a functionally graded Euler–Bernoulli beam model to treat a static problem of a simply supported beam [7].

Zhong and Yu presented exact solution for a cantilever FGB by considering it as an elasticity problem, the calculation involved is fairly cumbersome [8]. Chabraborty, *et al.* developed a new beam finite element to study the thermoelastic behavior of FGB [9]. Li, presented a unified approach for analyzing

Paper first received May.24, 2007 and in revised form July. 04, 2009.

G.H. Rahimi, is with the Department of Mechanical Engineering, Tarbiat Modares University, Jalal-e-Al-e-Ahmad Exp. Way, Tehran, Iran. Rahimi_gh@irost.org,
A.R, Davoodinik. is a PhD student at the same Department. Davoodinik@yahoo.com

FGB with the rotary inertia and shear deformation included. Then the free vibration of an FGB, where the dependence of the natural frequencies and mode shapes on the gradient index for a simply supported beam is given [10]. LI Yong-dong, *et al.* derived the Cauchy singular integral equation for the anti-plane fracture analysis of a functionally gradient material infinite strip with finite width, under the assumption that the shear modulus is an exponential function of the spatial coordinate [11]. Yang and Xiang investigated the static bending, free vibration, and dynamic response of monomorph, bimorph, and multimorph actuators made of functionally graded piezoelectric materials (FGPMs) under a combined thermal-electro-mechanical load by using the Timoshenko beam theory [12]. From the literature survey, it is seen that few studies have been made for an efficient discussion of the effect of temperature distribution on the thermal stresses and strains using Timoshenko beam theory for FGB. The objective of this paper is to present the responses of FGB under two types of thermal loads; the steady state of heat conduction with exponentially and hyperbolic variations through the thickness of FGB.

Firstly, the stability equations of beam will be derive by assuming thermal loading only based on the first order shear deformation theory (FSDT). Then the exact solution of the governing equations for FGB subjected to thermal load will be present. For verification of the procedure, The Euler–Bernoulli beam can be analytically reduced from the Timoshenko's beam theory.

Afterwards, with comparing of thermal behavior of both isotropic beam and FGB subjected to two functions of heat distributions, we will be study the effect of the type of temperature distribution on the thermal resultant distribution of stresses and strains. For evidence of the thermal behavior of FGB, first the same as function of material properties distribution and next, differ from that will be consider for function of heat distribution. Finally, results of the thermo-mechanical behavior of the FGB are presented and then conclusions are explained.

2. Material Gradient of FGM Beams

The FGM can be produced by continuously varying the constituents of multi-phase materials in a predetermined profile. The most distinct features of an FGM are the non-uniform microstructures with continuously graded macro properties.

An FGM can be defined by the variation in the volume fractions. Most researchers use the power-law function (P-FGM), exponential function (E-FGM), or sigmoid function (S-FGM) to describe the volume fractions [13]. In this study, properties distribution is defined by exponential function and method of problem solution can be extended for other type of distributions.

Consider an elastic rectangular cross section beam. As shown in Fig.1, coordinates x and y define the plane of the beam, whereas the z-axis originated at the middle surface of the beam is in the thickness direction.

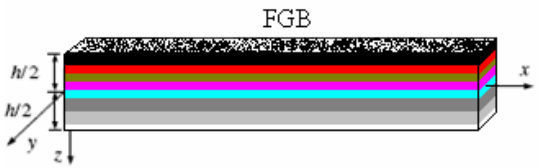

Fig.1. Elastic rectangular cross section FGB

Consider an E-FGB, with different exponential variations for distributions of thermal expansion, thermal conductivity and modulus of elasticity through the thickness direction of beam, respectively we have [1, 14];

$$\alpha_{(z)} = A_\alpha \cdot e^{\omega \cdot z}, A_\alpha = \sqrt{\alpha_1 \alpha_2} \quad , \omega = \frac{1}{h} \ln\left[\frac{\alpha_2}{\alpha_1}\right] \tag{1-a}$$

$$k_{(z)} = A_k \cdot e^{\beta \cdot z}, A_k = \sqrt{k_1 k_2} \quad , \beta = \frac{1}{h} \ln\left[\frac{k_2}{k_1}\right] \tag{1-b}$$

$$E_{(z)} = A_E \cdot e^{\lambda \cdot z}, A_E = \sqrt{E_1 E_2} \quad , \lambda = \frac{1}{h} \ln\left[\frac{E_2}{E_1}\right] \tag{1-c}$$

Where $(.)_1$, $(.)_2$ are the material properties in the z=-h/2, z=h/2 surfaces, respectively and the constants A_α, A_K, A_E, ω, β and λ can be obtained by boundary conditions (BCs). The kind of material properties distribution in the thickness direction of the E-FGB is plotted in Fig. 2.

3. Governing Equations

In accordance with the FSDT, a point A in the FGB with a distance z to the middle surface will be moved to point A' after deformation (Fig.3). Therefore, the axial displacement at the point A with distance *z* from mid-surface (*z*=0) can be presented by [15];

$$u(x,z) = u_0 - z\frac{\partial w}{\partial x} + z\phi_y \tag{2}$$

Where u_0 is the displacement at the middle surface and *w* is the transverse deformation, $\partial w/\partial x$ and ϕ_y are the rotations of vertical line AB (Fig. 3) about Y-axis due to bending and shearing deformations, respectively and all of them are independent of z-direction in FSDT [15].

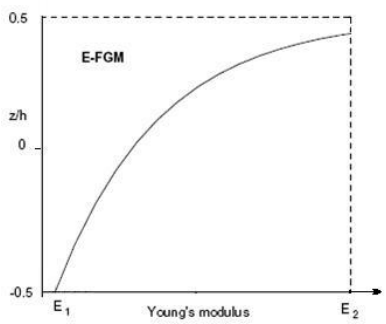

Fig.2. The Young's modulus distribution through the thickness direction of the E-FGB

Then strain in the x-direction as follows,

$$\varepsilon_{xx} = \frac{\partial u_0}{\partial x} - z\frac{\partial^2 w}{\partial x^2} + z\frac{\partial \phi_y}{\partial x} \tag{3}$$

Based on the plane strain condition, stress-strain relation for an FGB that subjected to thermal load is [16];

$$\sigma_{xx(z)} = \frac{E_{(z)}}{1-\nu}\left[\frac{\varepsilon_{xx}}{1+\nu} - \alpha_{(z)}T_{(z)}\right] \tag{4-a}$$

$$\sigma_{xx(z)} = \frac{E_{(z)}}{1-\nu^2}\left[\frac{\partial u_0}{\partial x} - z\frac{\partial^2 w}{\partial x^2} + z\frac{\partial \phi_y}{\partial x} - \alpha_{(z)}T_{(z)}(1+\nu)\right] \tag{4-b}$$

Where $\sigma_{xx(z)}$, ν and $T_{(z)}$ are the axial stress on the surface with distance *z* from mid surface, the Poisson's ratio and temperature distribution along z-direction of beam, respectively. As mentioned before, Eq. (4-b) has three unknown terms, which are independent of z-direction. These terms may be obtained by using the equilibrium equations and BCs.

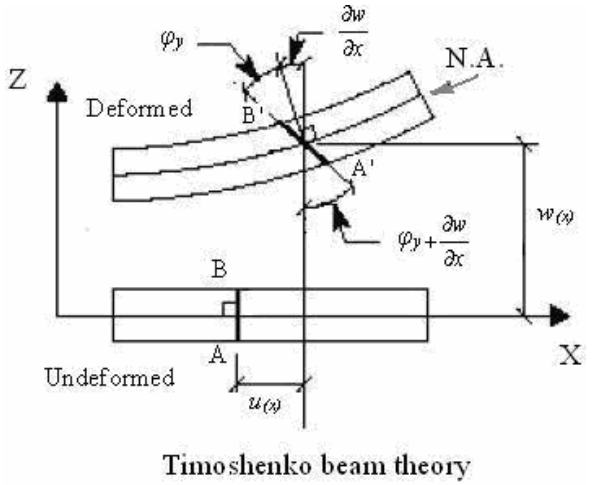

Fig.3. Axial, bending and shearing deformation characteristics of a beam according to FSDT

4. Problem Solution

4-1. Axial Stress

The stress resultants per unit length of the middle surfaces are defined by integrating stresses along the thickness. Assuming the thermal loading only with distribution in z-direction. When the beam is in equilibrium, the axial resultant forces in the x-direction must be zero, i.e.

$$\sum F_x = 0 \Rightarrow \int_{-h/2}^{h/2} \sigma_{xx(z)} b dz = 0, \quad 0 \le x \le l \tag{5}$$

Where, *b* and *l* are the width and length of beam, respectively. Moreover, in the absence of mechanical loads, the resultant moments about Y-axis appears by thermal effect only (M_{Ty}). Then the equilibrium equation for resultant moments as follows,

$$\begin{aligned} &\frac{\partial^2 w}{\partial x^2} I_y \int_{-h/2}^{h/2} E_{(z)} dz = -(M_{Ty} + M_{M_y}); \quad 0 \le x \le l \\ &M_{M_y} = 0; \quad 0 \le x \le l \end{aligned} \tag{6}$$

Where I_y that is the inertia moment and M_{Ty} are defined as follows [16];

$$I_y = \frac{1}{12} b h^3, \quad M_{Ty} = b \int_{-h/2}^{h/2} z E_{(z)} \alpha_{(z)} T_{(z)} dz \tag{7}$$

Moreover, M_{My} is presented the mechanical moment about Y-axis. Since there are three unknown terms in Eq. (4-b), we can provide the third equation with using BCs relation. The BCs of the simply supported FGM beam are;

$$w=0,\ M_y=0;\ x=0,\ x=l \tag{8-a}$$

$$\int_{-h/2}^{h/2} \sigma_{xx(z)} . z b dz = 0; \quad x = 0, x = l \tag{8-b}$$

Where M_y is the total moment acting on the beam about Y-axis. Then with collocation of Eq. (5), Eq. (6) and Eq. (8-b) the parameters u_0, $\partial w/\partial x$ and ϕ_y would be arisen and upon substitution into Eq. (4-b) axial stress can be obtained.

Consider conventional definitions for simplicity as follows,

$$\begin{aligned} &I_0 = \int_{-h/2}^{h/2} e^{\lambda . z} dz, \quad I_{0T} = \int_{-h/2}^{h/2} \alpha_0 \cdot e^{(\lambda+\omega)z} T_{(z)} dz, \\ &I_1 = \int_{-h/2}^{h/2} z . e^{\lambda . z} dz, \quad I_{1T} = \int_{-h/2}^{h/2} z \alpha_0 \cdot e^{(\lambda+\omega)z} T_{(z)} dz \\ &I_2 = \int_{-h/2}^{h/2} z^2 . e^{\lambda . z} dz, \quad I_{2T} = \int_{-h/2}^{h/2} z \alpha_0 \cdot e^{\alpha z} T_{(z)} dz \end{aligned} \tag{9-a}$$

$$C_1 = \frac{\partial u_0}{\partial x}, \quad C_2 = \frac{\partial^2 w}{\partial x^2}, \quad C_3 = \frac{\partial \varphi_y}{\partial x} \tag{9-b}$$

Where By substitution Eq. (9-a), Eq. (9-b), Eq. (7) and Eq. (4-b) into Eq. (5), Eq. (6) and Eq. (8-b) we can set the equation system with the following form;

$$\begin{cases} I_0 C_1 - (C_2 - C_3) I_1 = I_{0T} \\ I_1 C_1 - (C_2 - C_3) I_2 = I_{1T} \\ C_2 = \left(-I_{1T} \times b\right) / \left(I_y \times I_0\right) \end{cases} \tag{10}$$

Then the coefficient C_2 is directly obtained and for C_1, C_3 we have;

$$\begin{aligned} &C_1 = \frac{I_{1T} I_1 - I_{0T} I_2}{I_0 I_2 - I_1^2}, \\ &C_3 = \frac{-I_1 I_{0T} I_y I_0 + b I_0 I_{1T} I_2 - I_0{}^2 I_y I_{1T} - b I_1^2 I_{1T}}{I_y I_0 (I_0 I_2 - I_1^2)} \end{aligned} \tag{11}$$

It is evidence that axial stress can be obtain from Eq. (4-b) by substituting for C_1, C_2, and C_3 from Eq. (10) and Eq.(11) as follows;

$$\sigma_{xx(z)} = \frac{E_{(z)}}{1-\nu^2} \times \left[C_1 - zC_2 + zC_3 - \alpha_{(z)} T_{(z)} (1+\nu)\right] \tag{12}$$

4-2. Transverse Shear Stress

Consider an element of a FGM rectangular cross section beam of the length *dx*, and the width, *b*, as illustrated in Fig. 4. If the temperature distribution is assumed to be *T=T(z)*, the thermal bending takes place in the X-Z plane.

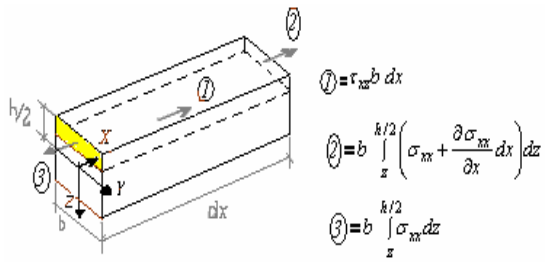

Fig.4. Transverse shear stress in the beam

The equilibrium equation for an element of the cross section of the FGB is:

$$\tau_{xz} b\, dx + b \int_z^{h/2} \left(\sigma_{xx} + \frac{\partial \sigma_{xx}}{\partial x} dx\right) dz - b \int_z^{h/2} \sigma_{xx} dz = 0 \tag{13}$$

, $-h/2 \le z \le h/2$

Where, τ_{xz} is the transverse shear stress. Rearranging the terms yields:

$$\tau_{xz} = -\int_z^{h/2} \left(\frac{\partial \sigma_{xx}}{\partial x}\right) dz \tag{14}$$

Substituting for σ_{xx} from Eq. (12), yields:

$$\tau_{xz(z)} = -\int_z^{h/2} \frac{\partial}{\partial x}\left[\frac{E_{(z)}}{1-\nu^2} \times \left(C_1 - zC_2 + zC_3 - \alpha_{(z)} T_{(z)} (1+\nu)\right)\right] dz \tag{15-a}$$

$$\tau_{xz(z)} = -\int_z^{h/2} \left[\frac{E_{(z)}}{1-\nu^2} \times \left(\frac{\partial^2 u}{\partial x^2} - z\frac{\partial^3 w}{\partial x^3} + z\frac{\partial^2 \phi_y}{\partial x^2} - \alpha_{(z)} T_{(z)} (1+\nu)\right)\right] dz \tag{15-b}$$

Tab. 1. Example of Material properties of E-FGM beam [16]

Material	ρ(Kg/m^3)	E(GPa)	ν	C_v(J/Kg°K)	k(W/m°K)	Melting point (°K)	α(/°K×10^{-6})
Al_2O_3	3970	393	0.3	775	30.1	2323	8.8
Ni	8900	199.5	0.3	444	90.7	1730	13.3

For FGB with simply supported ends the shear stress may be easily shown to be zero to causality of absent of second derivatives of u_0, ϕ_y and third derivative of *w*, while for FGB with fixed-simply supported ends lacking of shear stress is not accrued.

5. Procedure Verification

The Euler-Bernoulli beam theory is the special case of the beam theories. For verifying of mentioned method, we can ignore additional parameters of FSDT assumptions that compared with classical beam theory (CBT) and obtain same results.

In the event that intend the isotropic classical beam set forth for discussion, the parameters C_3 and ω, λ that presented for rotational deformation and non-isotropic properties, respectively, must be vanished. In addition, the Eq. (5) and Eq. (6) are satisfied incidentals to obtain the coefficients C_1, C_2.

These considerations and proper definition for heat distribution will be eventuated to same results of stress field for isotropic classical beam as is presented in some texts [17].

6.Steady state Temperature Distribution

6-1. Exponential Distribution of Temperature (E-State)

Assume the heat conduction is one-dimensional. If the exponential variation for coefficient of heat conduction through the thickness of E-FGB is considered as Eq. (1-b), the heat distribution in thickness direction, $T^e_{(z)}$, is;

$$T^e_{(z)} = A_{Te} + B_{Te} e^{\beta z} \tag{16}$$

Where constants A_T^e, B_T^e can be obtained from thermal BCs that are;

$$\textit{Thermal BCs}; \quad T_{(-h/2)} = T_1 \quad T_{(h/2)} = T_2 \tag{17}$$

$$A_{Te} = \frac{T_1 e^{\beta h} - T_2}{e^{\beta \cdot h} - 1}$$
$$B_{Te} = \left(T_2 - \frac{T_1 e^{\beta h} - T_2}{e^{\beta h} - 1}\right) e^{-\beta h} \tag{18}$$

Then with substitution of Eq. (18) in Eq. (16), we have;

$$T^{e}_{(z)} = \frac{T_1 e^{\beta h} - T_2}{e^{\beta h} - 1} + \left(T_2 - \frac{T_1 e^{\beta h} - T_2}{e^{\beta h} - 1} \right) e^{\beta (z-h)} \tag{19}$$

Finally with Eq. (12), Eq. (1-a) and Eq. (1-c), thermal stress can be obtained as follows;

$$\sigma_{xx(z)} = \frac{\sqrt{E_1 E_2}\, e^{\lambda \cdot z}}{1-\nu^2} \times \left\{ \left[C_1 - zC_2 + zC_3 \right] - \sqrt{\alpha_1 \alpha_2}\, e^{\omega \cdot z} (1+\nu)(A_{T^e} + B_{T^e} e^{\beta \cdot z} - T_0) \right\} \tag{20}$$

Where, T_0 is the stress free temperature.

6-2. Hyperbola Distribution of Temperature (H-State)

To study the impression of the temperature distribution type in the quality of thermal resultants distribution (TRD) of stresses, the hyperbola distribution of temperature also is considered. Therefore, with solving of one problem for two states of heat distribution, the responses of beam under these two conditions were comparable. Consider the hyperbola distribution of temperature as,

$$T^{H}(z) = \frac{T_2}{4} \left(\frac{2z}{h} + 1 \right)^2 \tag{21}$$

Where the temperature of boundary surface at z= h/2 is T_2= 300ºK and at z=-h/2 is zero.

7. Numerical Example

Consider an elastic rectangular cross section beam (Fig.1) with simply supported ends and dimensions b=h = 0.04(m).

Two types of beam theories with two types of beam constructions are exposed to two states of temperature distributions for driving the TRD of stresses and strains. The determination of thermal stresses distributions is established by CBT and FSDT for isotropic beam (kind of Ni, will be named as A-beam) and by FSDT for E-FGB (will be named as B-beam) with material properties that is presented in Table 1 [18].

If the temperature BCs are considered as follows:

$$T_0=0°K,\ T_1=0°K,\ T_2=300°K \tag{22}$$

Where T_0, T_1 and T_2 are indicated the temperature of stress free state, temperatures at surface z=-h/2 (unmixed Ni) and surface z=h/2 (unmixed Al_2O_3), respectively. Moreover, with consideration of material properties of B-beam (Table 1), for exponential terms in Eq. (20) we have:

$$E^* = e^{\lambda \cdot h} = \frac{E_{h/2}}{E_{-h/2}} = 1.97 \Rightarrow \lambda = 16.95 \tag{23-a}$$

$$\alpha^* = e^{\omega h} = \frac{\alpha_{h/2}}{\alpha_{-h/2}} = 0.6616 \Rightarrow \omega = -10.325 \tag{23-b}$$

$$k^* = e^{\beta \cdot h} = \frac{k_{h/2}}{k_{-h/2}} = 0.3318 \Rightarrow \beta = -27.575 \tag{23-c}$$

Then the I_y that is defined by Eq. (7), conventional definitions in Eq. (9-a) and E-state from Eq. (19) can be obtained as follows:

$$I_y=2.133E\text{-}7 \tag{24-a}$$

$$I_0=4.07E\text{-}2,\ I_1=9.144E\text{-}5,\ I_2=5.518E\text{-}6,\ I_{0T}=9.79E\text{-}5,\ I_{1T}=6.026E\text{-}7,\ I_{2T}=4.06E\text{-}7 \tag{24-b}$$

$$T^{e}_{(z)}=1149.017-149.017e^{(-27.575\, z+0.5515)} \tag{24-c}$$

Thus with substitution of Eq. (24-a) and Eq. (24-b) into Eq. (10) and Eq. (11), determination of C_1, C_2, and C3 are established, so that:

$$C_1 = \frac{\partial u_0}{\partial x} = 0.00224 \qquad C_2 = \frac{\partial^2 w}{\partial x^2} = -2.7711 \qquad C_3 = \frac{\partial \varphi_y}{\partial x} = -2.6990 \tag{25}$$

Now, with consideration of structural BCs as;

$$\varphi = u = \frac{\partial w}{\partial x} = 0; \quad x = \frac{l}{2} \qquad w = 0; \quad x = 0, x = l \tag{26}$$

determination of u_0, w and φ are achieved. In the interim of this numerical example, for transverse deformation, w, we have,

$$w = \frac{-2.7711}{2}(xl - x^2) \tag{27}$$

On the other hand, since the beam is thin, in the event that; if problem assumptions are varied to A-beam, same results will be obtained for FSDT and CBT in E-state (Table 2). Furthermore, in this numerical example the graphical results of H-state assumption will be presented for completion of discussion.

8. Results

8-1. Results for H-State

Consider the H-state in thickness direction of a beam as shown in Fig. 5. Whereas, with supposing that both A-beam and B-beam are exposed to H-state in thickness direction, similar response for TRD of stresses is achieved (Fig. 6). Indeed, the H-state in the thickness direction of B-beam is not operable, because the function of heat distribution must be same as function of material properties distribution. From Fig. 6 it is evidence that unlike material properties distribution, the kind of heat distribution is very affective in the quality of TRD of stresses.

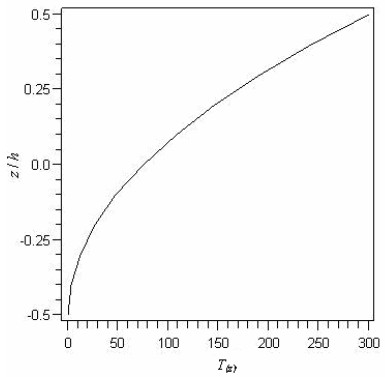

Fig. 5. Hyperbola distribution of temperature along the thickness direction of a beam

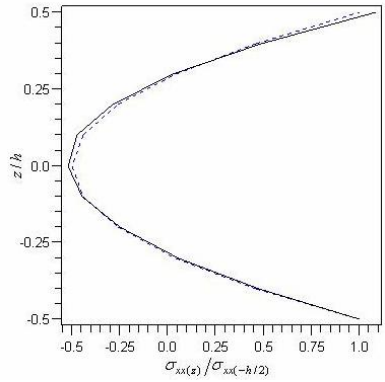

Fig.6. Non-dimensional TRD of stresses vs. thickness direction in H-state, dotted; A-beam, solid; B-beam

8-2. Results for E-State

With considering the E-state in thickness direction of a beam (Fig. 7), the TRD of stresses in thickness direction for both A-beam and B-beam are symmetrical with respect to z = 0 surface of the beams (resembling to H-state).

Fig. 8 is shown the TRD of stress in the both of them. It is clear that for both constructions of beam, TRD of stresses do not make any difference in these thermal BCs that is defined with Eq. (22).

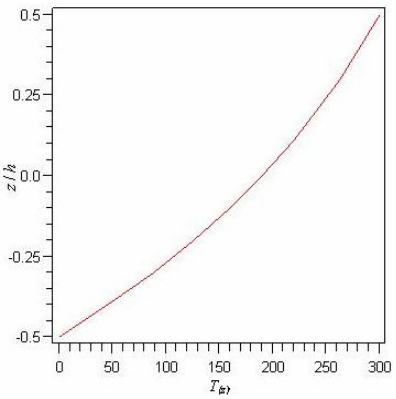

Fig.7. Exponentially distribution of heat in thickness direction of a beam

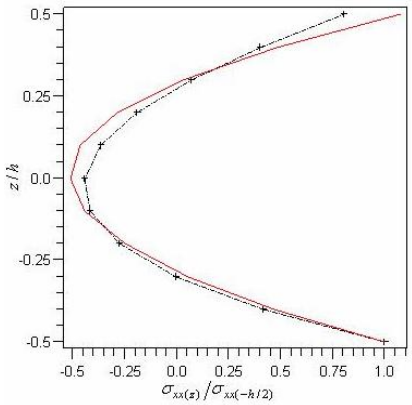

Fig. 8. Non dimensional TRD of stresses vs. thickness in E-state, dot line; Timoshenko's A-beam, cross; classical A-beam, solid line; B-beam ($Ni\text{-}Al_2O_3$)

Tab. 2. Results for Timoshenko's beam (FSDT) and classical beam (CBT) in E-state

	C_1	C_2	C_3	I_0	I_1	I_2	I_{0T}	I_{1T}	I_{2T}
FSDT	0.01166	-2.4446	-2.3468	0.04	0	5.33E-6	4.6658E-4	5.2151E-7	5.2151E-7
CBT	0.01166	-0.09778	0	0.04	0	5.33E-6	4.6658E-4	---*	5.2151E-7

*In CBT I_{1T} is vanished.

While, if with temperature increasing the new thermal BCs are defined as;

$$T_0=300^oK,\ T_1=700^oK,T_2=1000^oK \qquad (28)$$

Afterwards, the differences between TRD of stresses for A-beam and B-beam are entirely revealed (Fig. 9). In spite of this difference between them, they have same sign (positive) for thermal stresses in whole of the thickness. Because when temperatures are increased, increasing in tensile stresses that is arise from end supports effect, is larger from increasing in compression stresses that is result of thermal effect. Furthermore, whit equality of the subtraction of T_2 and T_1 in the Eq. (22) and Eq. (28), increasing in the tensile stresses (arising from end supports effect) with no changing in the compression stresses (arising from thermal effect) is happen.

9. Discussions

With separating the thermal responses of beams to two parts, the more analysis cases are available [16]. One part for explaining the thermal behavior of beam without any end supports (will be name as part A) and another part for representing the thermal behavior of beam with considering the end support influence (will be name as part B) when the beam is exposed to H-state or E-state. Thus for these two parts with

considering the Eq. (20), the following phrases can be obtained;

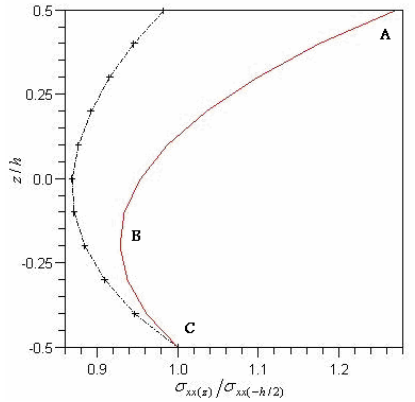

Fig. 9. Non dimensional TRD of stresses vs. thickness in E-state with high rate temperature, dotted; timoshenko A-beam, cross; classical A-beam, solid; B-beam (Ni-Al_2O_3)

$$\sigma^T = -\frac{\sqrt{E_1 E_2}\, e^{\lambda \cdot z}}{1-\nu}\left[\sqrt{\alpha_1 \alpha_2}\, e^{\omega \cdot z}\left(T^e_{(z)}\right)\right] \quad (29\text{-a})$$

$$\sigma^* = \frac{\sqrt{E_1 E_2}\, e^{\lambda \cdot z}}{1-\nu^2}\left[C_1 - zC_2 + zC_3\right] \quad (29\text{-b})$$

$$\varepsilon^T = \frac{\sqrt{\alpha_1 \alpha_2}\, e^{\omega \cdot z} T^e_{(z)}}{1-\nu} \quad (29\text{-c})$$

$$\varepsilon^* = \frac{\left[C_1 - zC_2 + zC_3\right]}{1-\nu^2} \quad (29\text{-d})$$

Where the σ^T, ε^T and σ^*, ε^* are the stress and strain resultants of part A and part B, respectively. Then the total stresses and strains are as follows;

$$\sigma = \sigma^* + \sigma^T \quad (30\text{-a})$$

$$\varepsilon = \varepsilon^* + \varepsilon^T \quad (30\text{-b})$$

Even now with Eq. (30-a) and Eq. (30-b) the distinctions of thermal behavior of A-beam and B-beam can be exactly specified.

In the H-state, Fig. 10 and Fig. 11 are shown the TRD of stresses and Fig. 12 and Fig. 13 are presented the TRD of strains for A-beam and B-beam, respectively.

Just as evidence, the distribution quality of part A and part B of stresses yield the symmetrically distribution of total stress. Furthermore, tensile stress (positive) is accrued in the inner section of thickness (-0.3<z/h<0.3) and the compression stresses is yield in the outer section of thickness (z/h<-0.3 & z/h>0.3). Now consider a beam with exposing to external pressure load on the one of boundary surfaces (i.e. z/h=-0.5). After bending of beam in H-state, the accumulation of thermal stress and mechanical stress in z/h=-0.5 surface is yield to increasing the coupling stresses and in the opposite side (z/h=0.5) decreasing of coupling stress is arisen. Therefore, in the H-state of thermal loading the outer surface of beam with bigger young modulus must be selected for subjecting to external pressure load. In the other hand, unlike the TRD of stresses, the TRD of strains is not symmetrical and after thermal bending the natural surface is appeared in z/h≈-0.325 with unsymmetrical final geometry for beam.

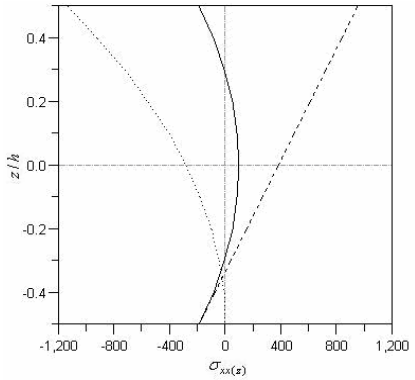

Fig. 10. TRD of stresses (MPa) vs. thickness in H-state for classical A-beam, dotted; stress resultants of part A (σ^T), dotted-dash; stress resultants of part B (σ^*), solid; total stresses (σ)

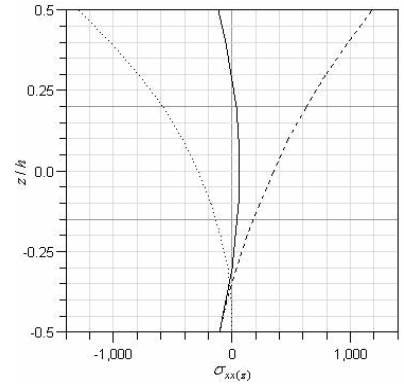

Fig. 11. TRD of stresses (MPa) vs. thickness in H-state for B-beam, dotted; stress resultants of part A (σ^T), dotted-dash; stress resultants of part B (σ^*), solid; total stresses (σ)

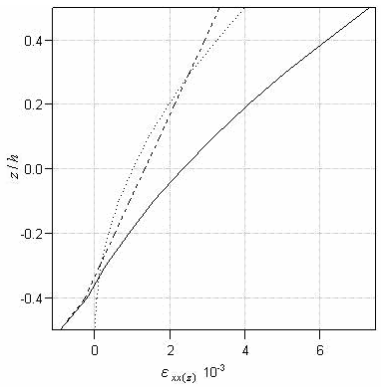

Fig. 12. TRD of strains vs. thickness in H-state for classical A-beam, dotted; strain resultants of part A (ε^T), dotted-dash; strain resultants of part B (ε^*), solid; total strains (ε)

When the B-beam is subjected to E-state, with thermal BCs corresponding to Eq. (22), TRD of stresses and strains would be as Fig. 14 and Fig. 15, respectively. According to them, an important point can be achieved that the neutral surface is vanished. In the other word, both the thermal stress and thermal strain are not contemporaneously equal to zero, and the thermal strains are always positive (tension mode) along thickness direction.

Furthermore, similar to H-state, the distribution quality of part A and part B of stresses yield the symmetrically distribution of total stress. Moreover, on the contrary to H-state, tensile stress (positive) is accrued in the outer section of thickness (z/h<-0.3 & z/h>0.3) and the compression stresses is yield in the inner section (-0.3<z/h<0.3). Now consider a beam with subjecting to external pressure load on the one of boundary surfaces (i.e. z/h=-0.5). After bending of beam in E-state, the accumulation of thermal stress and mechanical stress in z/h=-0.5 surface is yield to decreasing the coupling stresses and in the reverse side (z/h=0.5) the coupling stresses will be increased. Therefore, in the E-state for improving of beam responses, the outer surface of beam with smaller young's modulus must be selected for subjecting to external pressure load.

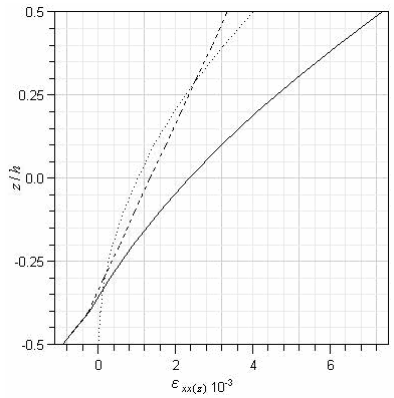

Fig. 13. TRD of strains vs. thickness in H-state for B-beam, dotted; strain resultants of part A (ε^T), dotted-dash; strain resultants of part B (ε^*), solid; total strains (ε)

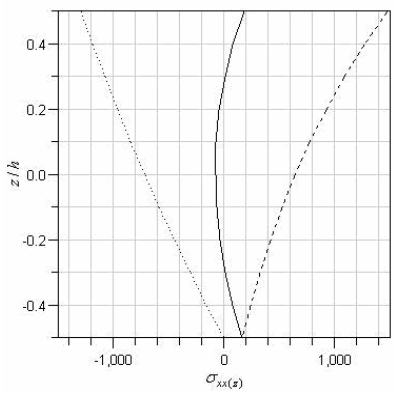

Fig. 14. TRD of stresses (MPa) vs. thickness in E-state for B-beam, dotted; stress resultants of part A (σ^T), dotted-dash; stress resultants of part B (σ^*), solid; total stresses (σ)

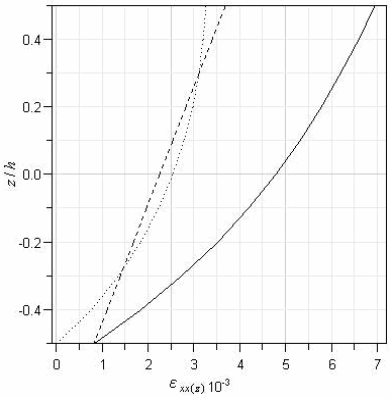

Fig. 15 TRD of strains vs. thickness in E-state for B-beam, dotted; strain resultants of part A (ε^T), dotted-dash; strain resultants of part B (ε^*), solid; total strains (ε)

10. Thermo-Mechanical Analysis

Consider the B-beam subjected to both external pressure load[2] on the one of boundary surfaces (i.e. z/h=-0.5) and E-state of thermal loading. Fig. 16 is comprised the superposition of thermal and mechanical stresses along the z-direction of B-beam.

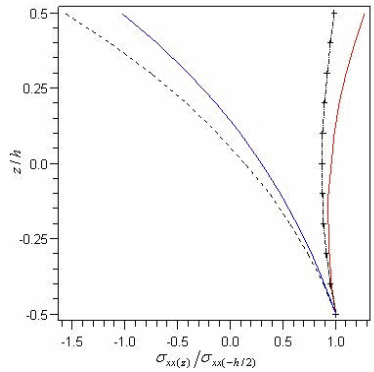

Fig. 16. Non dimensional stresses distribution vs. thickness for temperature boundary condition according to Eq.29 at the B-beam as exposed to thermo-mechanical load (E-state & External pressure on z/h=0.5), solid(right hand); thermal stresses, dotted(left hand); mechanical stresses, solid(left hand); total stresses

It is seen that in the outer section of B-beam thickness the thermal stresses is always positive (tensile stresses). Therefore, the summation of thermo-mechanical stresses is caused to improving the state of stress distribution with decreasing the compression stresses on the z/h=-0.5 surface. In the other hand, because of positive mechanical stress on the z/h=0.5 surface, increasing the total stress is appeared. Where as, in lower temperatures, that is caused the thermal stresses smaller than mechanical stresses, this increment is not considerable. Moreover, according to Fig.9, in higher temperatures the stresses distribution curve have two sections, one with smaller amount of

[2] *For details, see [15].*

slope that is appeared in larger section of thickness (section AB in Fig. 9) and another with larger amount of slope in smaller section (section BC in Fig. 9).

11. Conclusions

Some apposite conclusions can be demonstrated from this study as fallows;

- The quality of temperature distribution plays very important part in thermal resultant distribution of stresses for E-FGB. In the other words, for appearing the particular thermal behavior of FGB, the function of heat distribution must be same as function of material properties distribution. With supposing the hyperbola temperature distribution, it is no difference between thermal responses of isotropic beam and FGB.
- The thermal resultant distribution of stresses in the E-FGB with exponentially temperature distribution is on the contrary when compared with hyperbola temperature distribution. That means, in the outer sections of thickness the tensile stresses and in the inner sections of that the compression stresses is accrued.
- With temperature increasing in the exponentially temperature distribution state, the thermal stresses would gradually be as tensile stresses (positive) through the whole of thickness. Until, on the whole points of thickness direction the positive stresses is merely arisen.
- When the FGB is coincided to both external pressure load on the one of boundary surfaces and exponentially heat distribution with high temperature rate, for improving of total stresses distribution, the mechanical load must be applied on the side of thickness with smaller slope of thermal stresses distribution curve along of thickness.
- In lower temperature rate of exponentially heat distribution as the thermal stresses distribution is symmetrically respect to mid surface of FGB thickness, if it is also exposed to external pressure load on the one of boundary surfaces, for improving of total stresses distribution, the mechanical load must be applied on the side of thickness with weaker material properties.
- In the case of exponential distribution of thermal loading with no mechanical loads, in spite of the fact that the bending is accrued, the neutral surface does not come into existence.

References

[1] Javaheri, R., Eslami, M.R., *"Thermal Buckling of Functionally Graded Plates*", AIAA J;40(1):162–169, 2002.

[2] Najafizadeh, M.M., Eslami, M.R., *"First-Order-Theory-Based Thermo Elastic Stability of Functionally Graded Material Circular Plates*", AIAA J;40(7):1444–1450, 2002.

[3] Shen, H.S., *"Post Buckling Analysis of Axially Loaded Functionally Graded Cylindrical Panels in Thermal Environments*", Int J Solids Struct;39:5991–6010, 2002.

[4] Na, K.S., Kim, J.H., *"Three-Dimensional Thermal Buckling Analysis of Functionally Graded Materials*", Compos Part B, Eng; 35:429–437, 2004.

[5] Na, K.S., Kim, J.H., "*Three-dimensional thermo mechanical buckling analysis for functionally graded composite plates*", Composite Structures; 73:413–422, 2006.

[6] Ravichandran KS. "Thermal residual stresses in a functionally graded material system", Mater Sci Eng A; 201:269–276, 1995.

[7] Sankar, B.V., "*An Elasticity Solution for Functionally Graded Beams"*, Composites Science and Technology; 61:689–696, 2001.

[8] Zhong, Z., Yu, T., *"Analytical Solution of a Cantilever Functionally Grade Beam*", Composites Science and Technology; 67: 481–488, 2007.

[9] Chabraborty, A., Gopalakrishnan, S., Reddy, J.N., *"A New Beam Finite Element for the Analysis of Functionally Graded Materials"*, International Journal of Mechanical Science; 45: 519–539, 2003.

[10] Li, X.-F., *"A Unified Approach for Analyzing Static and Dynamic Behaviors of Functionally Graded Timoshenko and Euler–Bernoulli Beams*", Journal of Sound and Vibration; 318: 1210–1229, 2008.

[11] LI Yong-dong, JIA Bin, ZHANG Nan, DAI Yao, TANG Li-qiang, *"Anti-Plane Fracture Analysis of Functionally Gradient Material Infinite Strip with Finite Width*", Applied Mathematics and Mechanics; 27(6):773–780, 2006.

[12] Yang, J., Xiang, H.J., *"Thermo-Electro-Mechanical Characteristics of Functionally Graded Piezoelectric Actuators*", Smart Mater. Struct.; 16: 784–797, 2007.

[13] Shyang-Ho Chi, Yen-Ling Chung, *"Mechanical Behavior of Functionally Graded Material Plates Under Transverse Load-Part I: Analysis*", Inter. J. of Solids and Structures; 43: 3657-3674, 2006.

[14] Serkan Dag, Suat Kadioglu, O., Selcuk Yahsi, *"Circumferential Crack Problem for an FGM Cylinder Under Thermal Stresses*", J. of Thermal stresses", 22:659-687, 1999.

[15] Davoodinik, A.R., *"Mechanical Behavior Analysis of FGM Timoshenko's Beam*", Ph.D. dissertation, Tarbiat Modarres University, Tehran, 2005.

[16] Ugural, A.C., "*Stresses in Plates and Shells*", McGraw-Hill, New York, 1981.

[17] Nowinski, J.L., *"Theory of Thermo Elasticity with Applications"*, Sijthoff & Noordhoff International Publishers, 1978.

[18] Noack, J., Rolfes, R., Tessmer, J, *"New Layerwise Theories and Finite Elements for Efficient Thermal Analysis of Hybrid Structures*", Computers and Structures;81: 2525-2538, 2003